Argonne NATIONAL LABORATORY

Conference Paper Manuscript
APT#: 132165

Modeling the Ambient Condition Effects of an Air-Cooled Natural Circulation System

prepared by
Rui Hu, Darius Lisowski, Matthew Bucknor, Adam R. Kraus, Qiuping Lv

Nuclear Engineering Division
Argonne National Laboratory
9700 South Cass Avenue, Bldg. 208
Argonne, IL 60439-4854

25th International Conference on Nuclear Engineering
ICONE25
July 02 – 06, 2017
Shanghai
China

Proceedings of the 2017 25th International Conference on Nuclear Engineering
ICONE25
July 2-6, 2017, Shanghai, China

ICONE25-67418

MODELING THE AMBIENT CONDITION EFFECTS OF AN AIR-COOLED NATURAL CIRCULATION SYSTEM

Rui Hu
Nuclear Engineering Division
Argonne National Laboratory
Lemont, IL, USA

Darius D. Lisowski
Nuclear Engineering Division
Argonne National Laboratory
Lemont, IL, USA

Matthew Bucknor
Nuclear Engineering Division
Argonne National Laboratory
Lemont, IL, USA

Adam R. Kraus
Nuclear Engineering Division
Argonne National Laboratory
Lemont, IL, USA

Qiuping Lv
Nuclear Engineering Division
Argonne National Laboratory
Lemont, IL, USA

ABSTRACT

The Reactor Cavity Cooling System (RCCS) is a passive safety concept under consideration for the overall safety strategy of advanced reactors such as the High Temperature Gas-Cooled Reactor (HTGR). One such variant, air-cooled RCCS, uses natural convection to drive the flow of air from outside the reactor building to remove decay heat during normal operation and accident scenarios. The Natural convection Shutdown heat removal Test Facility (NSTF) at Argonne National Laboratory ("Argonne") is a half-scale model of the primary features of one conceptual air-cooled RCCS design. The facility was constructed to carry out highly instrumented experiments to study the performance of the RCCS concept for reactor decay heat removal that relies on natural convection cooling. Parallel modeling and simulation efforts were performed to support the design, operation, and analysis of the natural convection system.

Throughout the testing program, strong influences of ambient conditions were observed in the experimental data when baseline tests were repeated under the same test procedures. Thus, significant analysis efforts were devoted to gaining a better understanding of these influences and the subsequent response of the NSTF to ambient conditions. It was determined that air humidity had negligible impacts on NSTF system performance and therefore did not warrant consideration in the models. However, temperature differences between the building exterior and interior air, along with the outside wind speed, were shown to be dominant factors. Combining the stack and wind effects together, an empirical model was developed based on theoretical considerations and using experimental data to correlate zero-power system flow rates with ambient meteorological conditions. Some coefficients in the model were obtained based on best fitting the experimental data. The predictive capability of the empirical model was demonstrated by applying it to the new set of experimental data. The empirical model was also implemented in the computational models of the NSTF using both RELAP5-3D and STAR-CCM+ codes. Accounting for the effects of ambient conditions, simulations from both codes predicted the natural circulation flow rates very well.

INTRODUCTION

The Natural convection Shutdown heat removal Test Facility (NSTF) [1-3] is a large-scale thermal-hydraulics test facility that has been built at Argonne National Laboratory ("Argonne"). The facility was constructed to carry out highly instrumented experiments to validate the performance of the Reactor Cavity Cooling System (RCCS) concept for reactor decay heat removal that relies on natural convection cooling with either air or water-based systems.

The general facility layout is provided in Figure 1. A heat flux is applied to the back cavity wall by an array of electric radiant heaters, which leads to the development of a natural convection loop to cool the system. In a standard test, cold air is drawn from inside the building into the "downcomer" pipe and inlet plenum. Flow is then split between twelve riser ducts for the length of the heated cavity. These ducts all converge at an outlet plenum, where the flow mixes and is then exhausted from the NSTF through the two chimneys.

The scaling methodology has been developed in previous studies [1], which provides the background and similarity relationships that were derived to ensure preservation of key thermal-hydraulic behavior of the full-scale air-cooled RCCS design during the NSTF tests. Additionally, significant computational analyses [3, 4] have been performed for the NSTF to aid in its design, instrumentation, operation, and evaluation of its performance. Both system-level and computational fluid dynamics (CFD) codes were utilized in this effort. RELAP5-3D [5] and STAR-CCM+ [6] code evaluations were both conducted to provide the analytical basis for the NSTF to conduct scaled experimental simulations of the RCCS. It was concluded that the air-cooled RCCS could be simulated at the NSTF facility at a prototypic scale (a 19° sector slice) in the lateral direction and about half scale in the vertical direction.

The primary objective of the NSTF analyses is to assess the limitations in typical approaches for modeling this type of natural circulation RCCS system, and to validate the analysis methods and computer codes which may be used in licensing. Additionally, the NSTF analyses aided in the RCCS design optimization and supported experiment activities, i.e. helped to assure that the experimental procedures, setup, and measurements were performed as planned.

Significant efforts have been devoted to better understand the effects of weather conditions on NSTF system flow behavior. Strong influences of ambient conditions have been observed in the experimental results, when baseline tests were repeated several times under the same test procedures, yet the response of the system varied among the tests. The effects of air humidity, the building outside and inside temperatures, and the wind speed were investigated. A semi-analytical (or empirical) model was developed based on theoretical considerations and experimental data to correlate the zero-power system flow rates and the ambient conditions. The empirical model was also implemented in the computational models of the NSTF using both RELAP5-3D and STAR-CCM+ codes to examine its predictive capability.

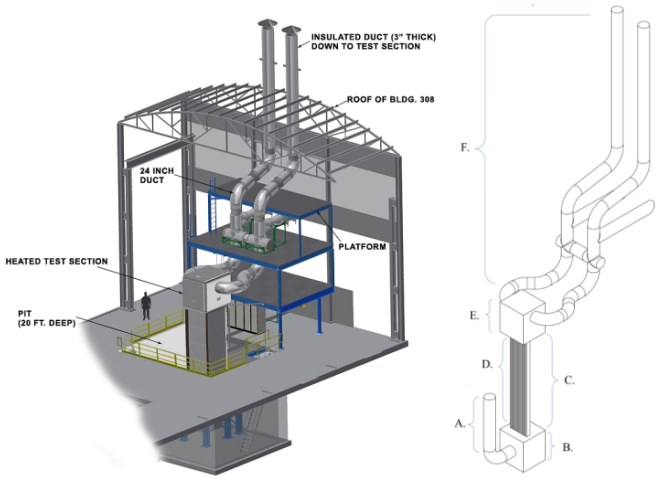

Figure 1: NSTF layout. Left: solid model rendering; Right: primary segments, A. inlet downcomer, B. inlet plenum, C. heated cavity, D. riser ducts, E. outlet plenum, F. chimney.

AMBIENT CONDITION EFFECTS

The NSTF is housed inside Building 308 at Argonne, with only the upper portion of the exhausting chimney ducts directly exposed to the outside environment. The presence of the building influences the ambient condition effects on the performance of the facility, which has been observed in the experimental data [7].

An example of these effects can be observed when comparing the experimental results of repeated baseline tests, which are shown in Figure 2. The baseline test case, as performed in the experimental testing program, was conducted on a regular basis to allow continuous monitoring of nominal facility behavior. Each test was performed in an identical facility configuration (uniform power profile, full elevation discharge via vertical chimney stacks) and in such a manner that maintained an equal time-power history across the test procedures. However, the performance of the system varied between the tests. Across the operational testing window, a total of eight baseline tests were conducted, with dates and outdoor temperature conditions summarized in Table 1. Across the eight runs, the observed outdoor temperature spanned -18.1 °C to 23.7 °C, or a total range of 41.8 °C.

A number of examinations were made to the multiple baseline test cases in an attempt to quantify and ascertain facility repeatability. Several metrics were used for comparison, e.g. thermal power within the test section determined by $\dot{m}C_p\Delta T$, where $\dot{m}$ is the total system flow rate, C_p is the specific heat determined at the average gas temperature, and ΔT is the difference between the gas temperatures at the outlet and inlet of the heated test section. Other metrics included as-measured temperatures, pressure drop, etc. At first glance of the measured thermal powers, Figure 2a, all test cases exhibit similar behavior and measured values fall within an acceptable variance (0.37 kW) from the sample mean (49.45 kW).

However, further examination of additional parameters, such as the heated section air temperature rise (Figure 2b) and the system mass flow rate (Figure 2c), indicate large differences across the different runs. Isothermal forced flow testing was performed on a regular basis and indicated that frictional losses, e.g. due to geometric changes, had not changed within the bounds of experimental uncertainty. The ambient conditions (outside temperature and wind) and the building interior temperature are likely the dominant factors.

Table 1: Overview of repeatability testing at baseline conditions

Test No.	Dates Performed	Outdoor Temperature, °C		
		Average	Minimum	Maximum
Run003	03/10–12/2014	n/a	n/a	n/a
Run004	04/09–11/2014	13.9	10.2	17.1
Run011	01/28–30/2015	2.09	1.40	2.80
Run020	09/05–07/2015	23.3	22.5	23.7
SPEF003	10/12–19/2015	11.5	11.1	12.2
Run022	01/17–22/2016	-17.6	-18.1	-16.8
Run024	04/08–14/2016	5.3	-4.90	17.3
Run026	05/16–20/2016	13.6	5.80	21.6

The natural draft of air was continuously observed before power was turned on in NSTF experiments. As discussed in Ref. [8], the natural ventilation by air inflow and outflow depends on the size and location of all air leakage sites on the building envelope and the indoor-outdoor pressure difference across each of these sites. These pressure differences are the result of a non-linear interaction between wind pressures on the exterior of the building and stack effect pressures caused by the density difference between indoor and outdoor air. The independent wind and stack effects would naturally interact to set the building indoor pressure that maintains a balance between the overall inflow and outflow mass flow rates across the building envelope.

Considering the uncertainty in estimating wind shelter effects and in determining the distribution of leakage sites, an analytical study of the combined wind and stack effect in Building 308 (which houses the NSTF) would be very challenging. The location of leakage on the building envelope determines the wind and stack pressures that occur across each leakage site. Therefore, it was proposed to measure the airflow rates in the NSTF system under zero-power and a wide range of wind and outside air temperature conditions. By relying on a large database of airflow rates, an empirical relationship was developed between the NSTF airflow rates and the ambient conditions.

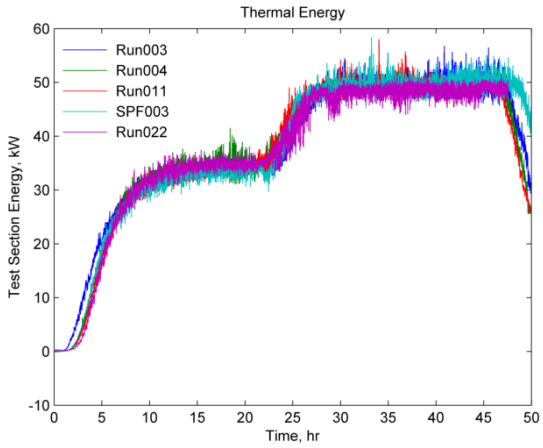

(a) Thermal energy removed by air in risers

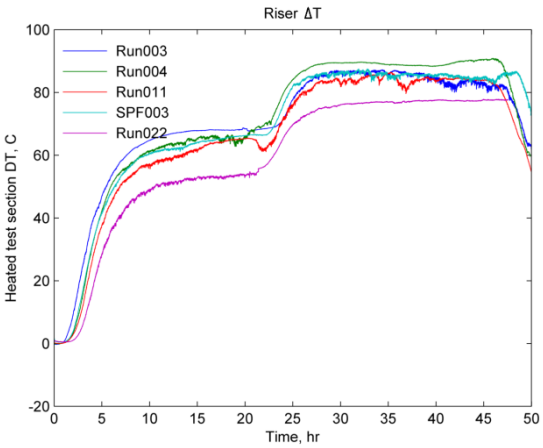

(b) Air temperature increase in risers

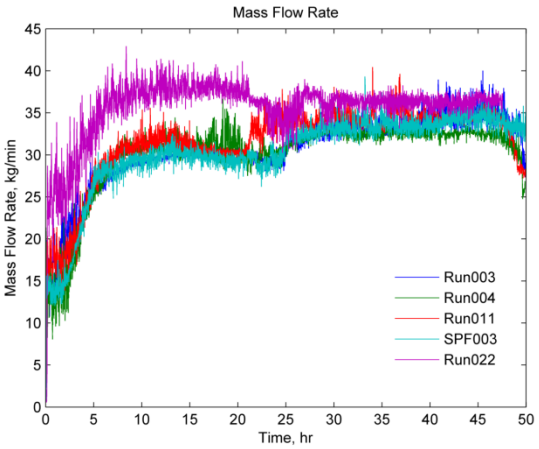

(c) Mass flow rates

Figure 2: Repeatability of NSTF baseline tests.

Stack- and Wind-Effect Pressures

Figure 3A illustrates the linear change of stack pressure with height (assuming linear change of air density due to temperature change for illustration purpose), h, given by

$$P_s(h) = \rho_{out} g h \frac{T_{in} - T_{out}}{T_{in}} \quad (1)$$

where the maximum pressure is P_{stack} (at $h = H$). This figure is for the case when $T_{in} > T_{out}$. The sign of the pressure is reversed for $T_{in} < T_{out}$. In order to balance the flows in and out of the building there is a pressure shift inside the building ($P_{s,i}$) that results in the pressure variation shown in Figure 3B. This would result in outflow through the upper part of the building (chimney outlet) and inflow in the lower part. At the neutral level height $h_{o,s}$, dependent upon the leakage distribution, there is no pressure difference across the wall. The pressure difference across the structure then varies linearly with height, which results in flow distributions illustrated in Figure 3C.

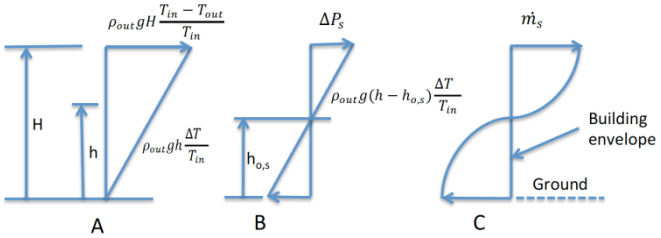

Figure 3: Stack effects on pressure and flow. A: (stack pressure head), B: (pressure difference), C: air infiltration mass flow.

The wind would also affect the air infiltration dependent on the leakage distribution, pressure coefficients, and inflow and outflow balance. In general, wind flowing over the top of a chimney can increase the draft by producing a driving low pressure region that assists in pulling air from the chimney. However, under different geometric configurations and wind directions, the wind can be adverse to the chimney upward flow by creating positive pressure at the top of the chimney. The wind blowing around a building produces a positive pressure zone on the windward side and a negative pressure zone on the leeward side. These pressures act on the leaks in the building envelope, causing airflow through them and changing the pressures within the building. Assuming the largest leakage path in Building 308 is through the NSTF chimney outlet, the wind would always enhance the flow in NSTF tests. The wind influences on the building envelope pressure and NSTF air flow rate are illustrated in Figure 4.

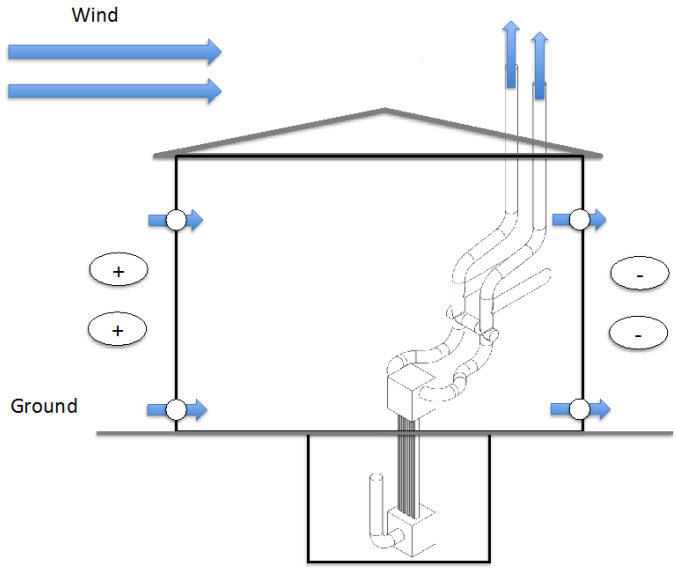

Figure 4: Wind effects to air infiltration in Building 308 and NSTF system flow.

The wind effect on the driving pressure (pressure difference between inside and outside of the building) for NSTF flow can be modeled as:

$$\Delta P_w = C_w P_{wind} = \frac{C_w \rho_{out} V_w^2}{2} \quad (2)$$

In which C_w is the wind effect factor, and V_w is the wind speed.

A Semi-Analytical Model of Stack and Wind Effects

Combining the stack and wind effects together, the total additional driving pressure can be modeled as:

$$\Delta P_{total} = P_s + \Delta P_w = \beta \rho (T_{in} - T_{out}) g H + \frac{C_w \rho_{out} V_w^2}{2} \quad (3)$$

in which β is the air expansion coefficient, and H is the height between the NSTF chimney outlet and the ground. This approach models the full air flow path from the outside of the building, infiltrating to the inside of the building at the ground level, entering into the NSTF downcomer, and passing through NSTF piping, and leaving the NSTF duct system through the chimney outlets. The total driving force would be balanced by the pressure losses in all parts of the system. The total pressure loss can be correlated with the system flow rate:

$$\Delta P_{loss} = C_l \dot{m}^n = \sum \left(K_i \frac{1}{2} \rho v_i^2 + f_j \frac{L_j}{D_j} \frac{1}{2} \rho v_j^2 \right) \quad (4)$$

in which K_i is the form loss coefficient, and f_j is the friction coefficient. Combining Eqs. (3) and (4), we have:

$$C_l \dot{m}^n = \beta \rho (T_{in} - T_{out}) g H + \frac{C_w \rho_{out} V_w^2}{2} \quad (5)$$

or

$$\dot{m}^n = C_s' (T_{in} - T_{out}) + C_w' V_w^2 \quad (6)$$

in which

$$C_s' = \frac{\beta \rho g H}{C_l} \quad (7)$$

$$C_w' = \frac{C_w \rho_{out}}{2C_l} \quad (8)$$

The values of the empirical coefficients C_s', C_w', and the exponent n $(1 < n < 2)$ can be determined from the NSTF zero-power test results. For orifice-type resistance such as holes, we expect $n = 2$ (constant form loss coefficient). For long channels the lower limit on n is the fully-developed laminar flow condition $n = 1$, as $f = \frac{C}{Re}$. For the flow rates observed in the NSTF riser ducts, the flow is always turbulent. For the Reynolds number range observed, the exponent n should be 1.75 if the Blasius friction factor correlation [9] is considered,

$$f = 0.316\mathrm{Re}^{-0.25}. \quad (9)$$

Combining the effects from both the form losses $(n = 2)$ and friction losses $(n = 1.75$ for turbulent flow and $n = 1$ for laminar flow), and considering the dominant pressure loss in the whole system is the turbulent friction loss in the riser ducts $(n = 1.75)$, n was chosen to be equal to 1.8, and experiment data was used to determine the coefficients C_s' and C_w'.

$$\dot{m} = (C_s' \Delta T + C_w' V_w^2)^{5/9}. \quad (10)$$

The result will provide a physical basis for predicting the induced flow rate as a function of ambient temperature and wind conditions.

Relevant data generated at zero power conditions were compiled and prepared into a format that would allow fitting of these two coefficients. These data sets included pre-testing zero flow values, along with an additional separate effects test SPEF005 conducted without electric heating. The span of available data is summarized in Table 2. The measured flow rate and ambient wind speed from the separate effect test SPEF005 are shown in Figure 5. Even without active heating, the driving pressure differences, caused by density differences (stack effects) and augmented by the wind, create a natural draft through the NSTF.

Table 2: Span of available data collected at zero power conditions

	T_{inlet} (°C)	$T_{outdoor}$ (°C)	ΔT (°C)	Wind Speed (m/s)	Flow Rate (kg/min)
Minimum	15.85	-16.7	0.44	0.04	0.12
Maximum	25.77	27.97	32.93	11.20	37.19

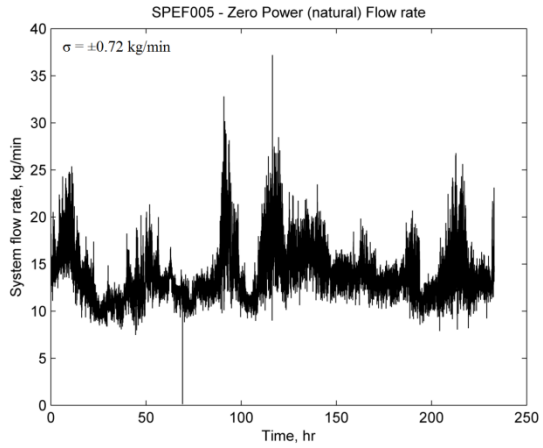

(a) Measured flow rate

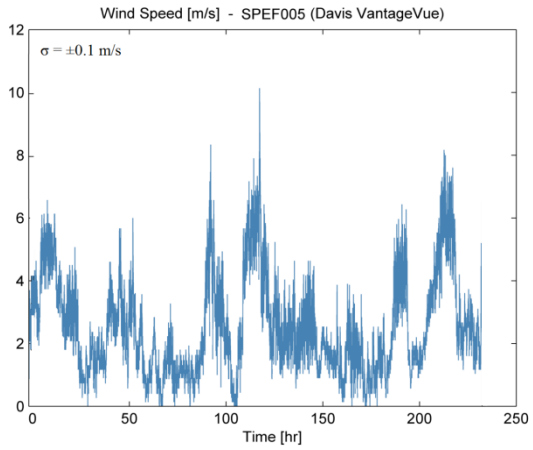

(b) Ambient wind speed

Figure 5: Measured flow rates and wind speed in SPEF005.

A fitting program was scripted in MATLAB [10] that iterated over values of constants C_s' and C_w', compared the resulting mass flow rate against actual values, and identified best fit values based on a minimum root-mean-squared-error (RMSE). Both constants were given a range from 0 to 20 at 0.01 increments. The results determined that best-fit values for C_s' and C_w' were 5.53 and 3.75, respectively.

$$\dot{m} = (5.53\,\Delta T + 3.75\,V_w^2)^{5/9}. \quad (11)$$

A response surface was generated showing the calculated flow rate as a function of temperature and wind speeds, as shown in Figure 6.

The correlation was then compared first against the test data from SPEF005, shown in Figure 7. Given that this data were included in determining the constants, the high level of agreement is expected. To ensure validity of this predicative capability, a new test (SPEF007) was performed in the test facility that generated data not used in the fitting correlation. The results are shown in Figure 8, further confirming validity and confidence in the findings. The goodness of the fit between the correlation and measured data were further confirmed by the RMSE of 0.79 kg/min and 0.66 kg/min for SPEF005 and SPEF007, respectively. This is deemed very good considering

that the measurement uncertainty of mass flow rate is 0.72 kg/min. The R^2 values of the comparisons between the correlation and measurements were 0.87 for SPEF005 and 0.93 for SPEF007.

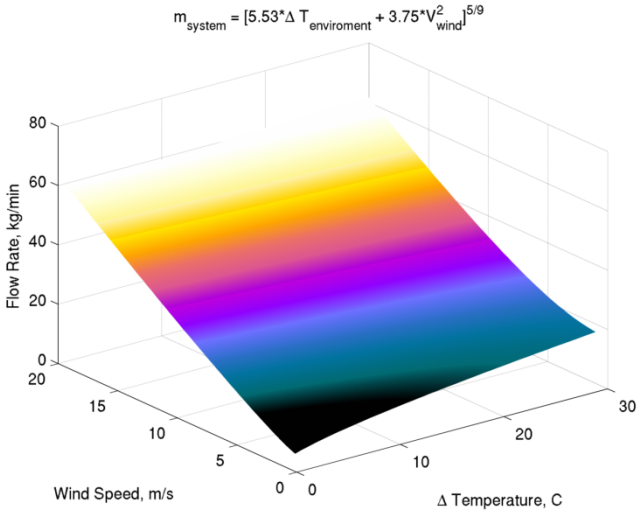

Figure 6: Response surface of fitting correlation.

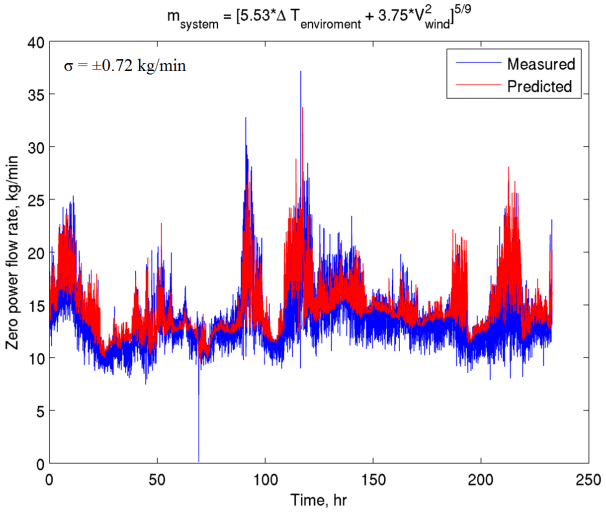

Figure 7: Fitting correlation applied to SPEF005.

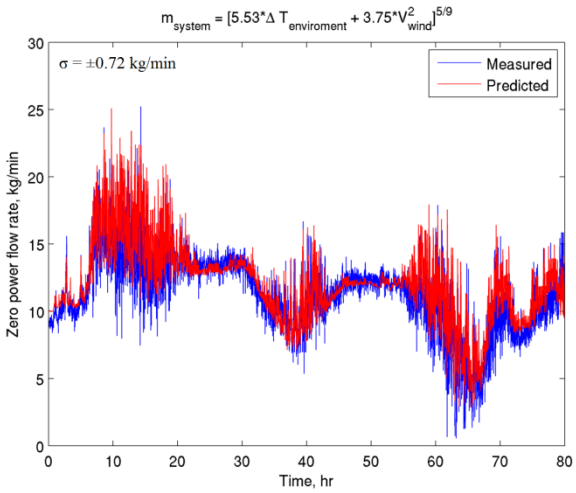

Figure 8: Fitting correlation applied to SPEF007.

Building Temperature Effects

The differences in the baseline tests can also be partially attributed to changes in the building temperature. This effect can be described as follows: the driving pressure head of a natural circulation system is highly dependent on the density difference between the cold and hot segments. Given the non-linear relationship between density and temperature for an ideal air gas, Figure 9, the absolute inlet temperature plays a role, even for two systems with identical temperature differences. With higher absolute inlet temperatures, the $\Delta\rho/\Delta T$ is reduced, which lowers the driving pressure head and reduces the overall efficiency of the stack effect.

Thus, with elevated downcomer inlet temperatures causing a reduction in the driving head, the mass flow rate is reduced, and to maintain equal thermal powers, all of the system parameters shift. Specifically, the air temperature rise increases, absolute gas temperature increases, frictional pressure drop decreases, etc. The inlet temperature effect can be easily captured by applying realistic air property models in the computational models.

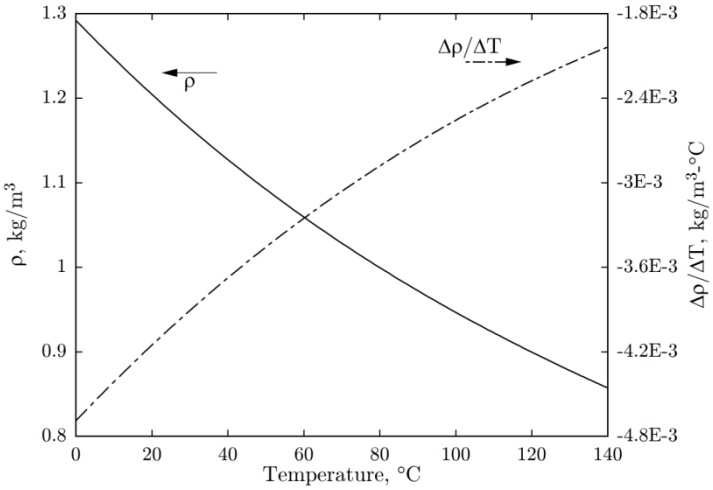

Figure 9: Relationship between density and temperature for air.

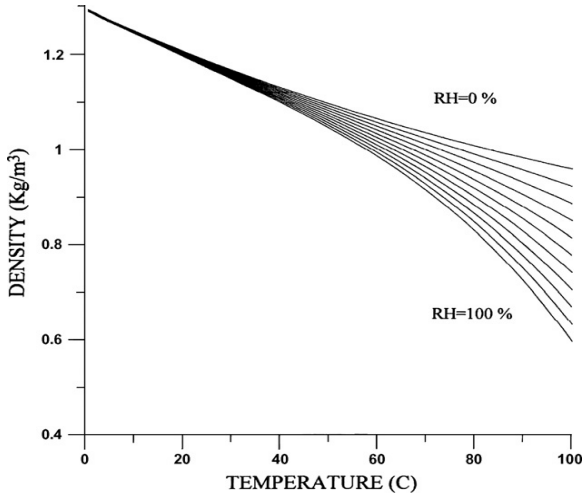

Figure 10: The moist air density as a function of temperature with the relative humidity [11].

Air Humidity Effects

In NSTF tests, the outdoor relative humidity (RH) was observed to span between 25 and 98%. The impact of air humidity on NSTF system behavior was also evaluated. Figure 10 [11] shows the moist air density as a function of temperature for an increasing RH from the minimum value of 0%, corresponding to dry air (top curve), up to the maximum value of RH = 100% (lower curve), corresponding to saturated conditions, in 10% steps. The increase of RH leads to a decrease of humid air density, especially at the range of higher temperatures. While an RH increase between 0 and 100% leads to an almost negligible density decrease of humid air at near freezing temperatures, it is responsible for a significant reduction of humid air density of about 37.5%, at temperatures close to 100 °C.

Similar findings were found for other properties of the humid air, i.e. when the temperature is low, the increase of RH has negligible impacts on the air properties. This is expected as the low temperature air can only absorb very limited content of water vapor in the air. Figure 11 shows the change of RH with the increase of temperature. If the NSTF air has 80% RH and 20 °C air at the downcomer inlet, by the time it heats up and leaves the risers at ~100 °C its RH is less than 2%. The effects of air humidity were also investigated using RELAP5-3D simulations of Run020. Figure 12 compared the calculated mass flow rates of the system for Run020 with dry air and with saturated air. The maximum difference between the two cases in mass flow rates is approximately 2%. Note that Run020 has the highest inlet temperature for all baseline tests, yet the differences between the results for saturated air and dry air are very small. It therefore can be concluded that the air humidity would only have negligible impacts to NSTF system behavior, and does not need to be considered in the computational models.

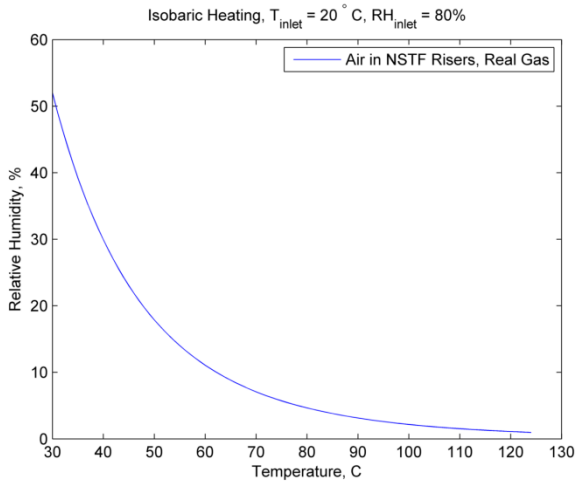

Figure 11: The relative humidity as a function of temperature with inlet air at 80% RH and 20 °C.

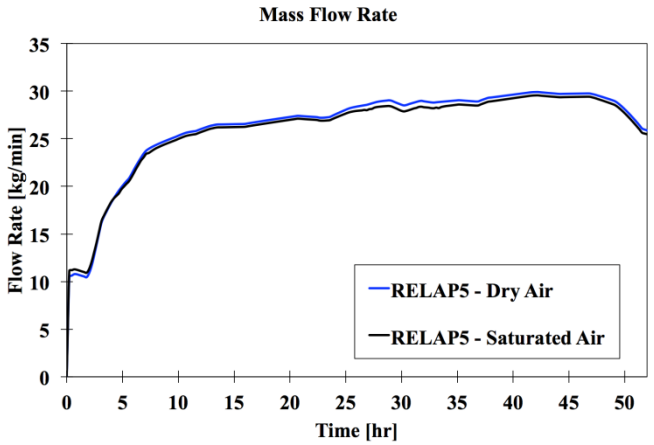

Figure 12: The effects of humidity on the system flow rate, RELAP5-3D simulations of Run020.

APPLICATION OF THE SEMI-ANALYTICAL MODEL

As part of the modeling effort conducted during this project, a RELAP5-3D model was developed for the NSTF to perform transient analysis and focused primarily on simulating the integral system performance of the facility. To analyze the ability of the model to predict important performance metrics of the facility (such as the air mass flow rate), comparisons were made between experimental test data and code simulation results.

After initial comparisons and the assessments [12] of the experimental results of several repeated baseline tests, it became apparent that modeling ambient effects on the facility would be necessary to properly simulate the overall system performance. To simulate these conditions in the model, virtual volumes were added to account for the temperature effects on the facility, while wind effects were simulated by controlling the pressure difference between the inlet and outlet of the facility based on Eq. (2).

The RELAP5-3D model, Figure 13, was calibrated to results from a single experimental test (Run022) to accurately account for flow resistances in the facility as well as air entering the NSTF building. Following calibration, the model was used to simulate additional experimental tests (Run011, Run020, and Run024) over a range of operating and ambient conditions. The simulation results compared well with experimental data for all of the tests for the overall system mass flow rate (the average absolute error was less than 5% in all of the simulations). These simulation results demonstrate that the integral behavior of the system were well captured and the effects of ambient conditions were correctly modeled (for outdoor temperatures ranging from -22.3 °C to 33.4 °C and wind speeds ranging from 0 m/s and 8.5 m/s).

Simulation results for Run022 are provided in Figure 14. Simulation results for the "No Wind/Temperature" are provided to demonstrate the importance in capturing the effects of outside air temperature and wind of the facility. If these effects were neglected, the simulation results significantly under-predicted the mass flow rate of the facility.

If the effects of outdoor air temperature on the performance of the facility are modeled, the results provide better agreement in mass flow rate to the experimental data. If the wind effects are also modeled, the average absolute error between the simulation and the experimental data is less than 2%, which is about the same as the measurement uncertainty. It should be noted that the wind speed is very low from 40 hours to 120 hours in the test. Prior to 40 hours, significant wind effects were observed in the experimental data. In this region, the simulation results with no wind effects modeled under-approximate the mass flow rate of the system (the average absolute error is less than 5%). The simulation results where several peak wind speeds were also included to demonstrate that the simulation can capture the peak mass flow rates in the experiments if the detailed variation of wind speeds were modeled in the simulation. It should be noted that the average wind speed plus peak simulation results do not correspond to the highest experimental data points because the data collected by the weather station was actually being averaged during data acquisition. The weather station sampled wind speed several times a minute, but only records a 1-minute average and a peak value during that 1-minute time period. Therefore, the peaks seen in the experimental wind data are lower than the true peak wind speed during the same timeframe. For example, the highest 1-minute-averaged wind speed measured by the weather station during Run022 was 8.5 m/s, however, the actual peak wind speed was measured to be approximately 12 m/s.

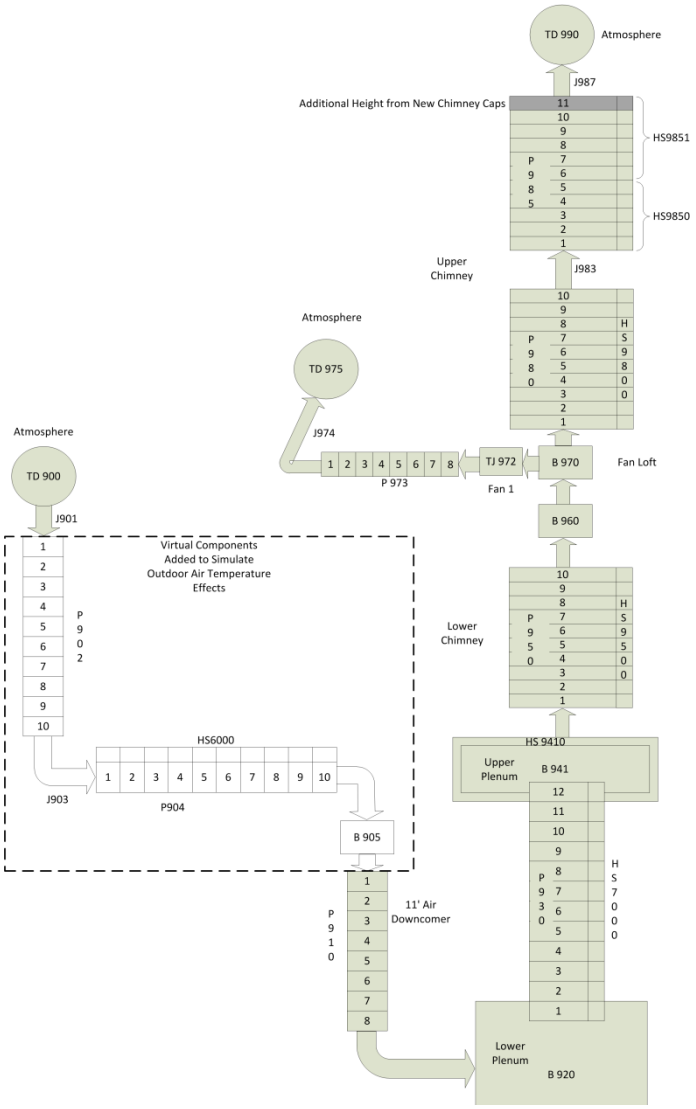

Figure 13: Nodalization diagram of NSTF model in RELAP5-3D.

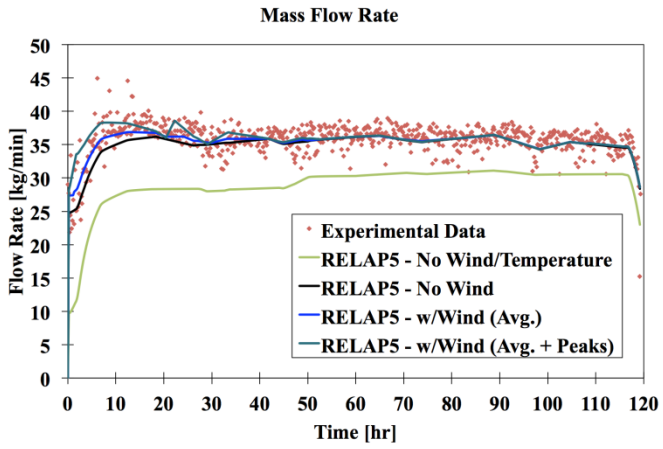

Figure 14: Comparison of RELAP5-3D simulation results and experimental data.

The three-dimensional modeling of the NSTF was performed using the computational fluid dynamics (CFD) code STAR-CCM+ version 10.06 [6]. Earlier works published [13, 14] by the authors provide the background, geometry, and the turbulence modeling details of the CFD model. All CFD simulations performed within this work were steady state, with the objective of capturing the mean behavior of the system for a given power level. It was found in previous simulations of Run022 that the mass flow rate was under-predicted in the computational results, notably in the low power case. Accounting for the outside weather effects could increase the flow rate in these cases. The outside temperature is significantly lower than the inside temperature during the steady-state periods in Run022, which will create a positive pressure head due to the stack effects in the NSTF building.

The theoretical basis of the weather effects is described above. However, some adjustments are needed to apply it to the CFD model. The main issue is that there are significant pressure losses that are not modeled in the CFD model shown in Figure 15, notably the substantial losses for air leaking into the building. Thus the net pressure head must be modified to:

$$\Delta P_{net} = P_s + \Delta P_w - \Delta P_{loss} \qquad (12)$$

$$= \rho\beta(T_{in} - T_{out})gH + \frac{C_w \rho_{out} V_w^2}{2} - \frac{K}{2}\rho_{in} V_{in}^2 ,$$

where K is the loss coefficient representing the building losses. In the CFD model, this loss is applied as a porous baffle in STAR-CCM+. The two left-most terms in ΔP_{net} are calculated based on the weather data and applied as a boundary condition at the pressure inlet. An appropriate value for the loss coefficient was calculated from forced-flow simulations.

The difference in piezometric pressure [6] between the domain inlet and outlet was obtained for both the high and low power cases. As an illustration, if the piezometric pressure difference were zero, this would mean that the mass flow rate would be completely governed by the buoyancy source from the heated plate and the pressure losses of the NSTF. Thus, the weather and loss effects would cancel. If there was a higher piezometric pressure at the inlet, it means that the weather effects produce a positive pressure head in excess of that subtracted by the form pressure loss at the inlet. The piezometric difference can be regarded as ΔP_{net} in Eq. (12).

The effects on mass flow rate from applying the weather modeling are provided in Table 3. The impact shown on mass flow rate demonstrates that the weather modeling improves the flow rate estimates, particularly for the low power case in which significant ambient condition (high wind speeds and low outdoor temperature) effects were observed in the experiment.

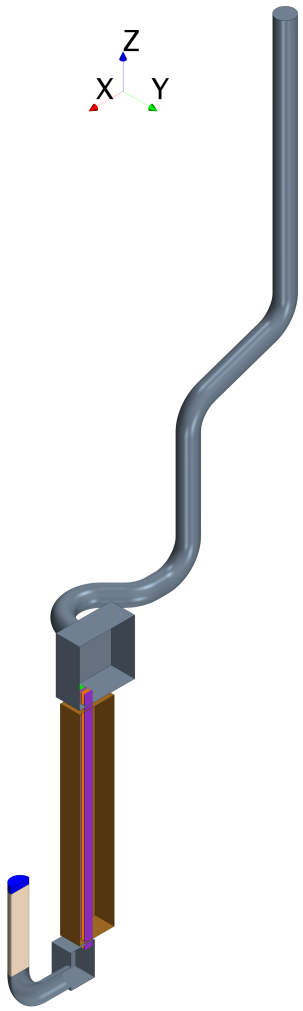

Figure 15: NSTF model in STAR-CCM+.

Table 3: Mass Flow rate comparisons for natural convection simulation cases

	High Power			Low Power		
	Experi-ment	CFD - w/o weather	CFD - weather effects	Experi-ment	CFD - w/o weather	CFD - weather effects
$\dot{m}$ (kg/s)	0.606	0.604	0.608	0.595	0.543	0.585
Difference (%)	-	0.3	0.3	-	8.7	1.7

CONCLUSIONS

Highly instrumented experiments have been performed at NSTF to study the performance of the air-cooled RCCS concept for reactor decay heat removal that rely on natural convection cooling. Parallel modeling and simulation efforts were performed to support the design, operation, and analysis of the natural convection systems. As strong influences of ambient conditions were observed in the experimental results, significant efforts were devoted to improve the understanding of the weather effects on NSTF system flow behavior.

It was determined that air humidity had negligible impacts on NSTF system behavior and therefore did not warrant consideration in the models. However, temperature differences between the building exterior and interior air, along with the outside wind speed, were shown to be dominant factors. An empirical model was developed based on theoretical considerations of the stack pressure effects and the wind effects on system flow rates, while some coefficients in the model were obtained based on best fitting the experimental data. The predictive capability of the model is demonstrated by applying it to a wide range of zero-power test data.

The empirical model has been also implemented in the computational analyses of NSTF tests using both the system code RELAP5-3D and CFD code STAR-CCM+. It is demonstrated that both codes can accurately simulate the integral behavior of the system responses at the NSTF if the effects of ambient conditions are modeled or accounted for. Very good agreement was found between the simulation results and experimental data. This helped to assure high confidence in NSTF experimental data that can be used to support the design and licensing of an RCCS in advanced reactors, and strengthened the ability of analysis to accurately model the observed physical behavior. Note that the derivation of the empirical model and the modeling approaches used in RELAP5-3D and STAR-CCM+ to capture the ambient condition effects can be applied in the computational modeling of other air-cooled natural circulation systems.

NOMENCLATURE

C_w,$C_w{}'$: Wind effect coefficient
$C_s{}'$: Stack effect coefficient
D: Hydraulic Diameter (m)
f: Friction coefficient
g: Gravity acceleration (m/s^2)
H, h: Height (m)
K: Form loss coefficient
L: Length (m)
$\dot{m}$: Flow rate (kg/s)
P: Pressure (Pa)
P_s, P_{stack}: Stack pressure effect (Pa)
P_w: Wind pressure effect (Pa)
ΔP: Pressure drop (Pa)
Re: Reynolds number
T: Temperature (K)
ΔT: Temperature Difference (K)
V_w: Wind speed (m/s)
ρ: Density (kg/m^3)
β: Thermal expansion coefficient, (1/K)

Subscripts
in: System inlet
out: System outlet
s: Stack
w: Wind
net: Net effective
loss: Loss

ACKNOWLEDGMENTS

This work was supported by the U.S. Department of Energy Office of Nuclear Energy, Office of Advanced Reactor Technology, under Contract No. DE-AC02-06CH11357. The authors gratefully acknowledge the use of the Blues cluster at the Laboratory Computing Resource Center at Argonne National Laboratory.

REFERENCES

[1] S. Lomperski, W.D. Pointer, C.P. Tzanos, et al., 2011, "Generation IV Nuclear Energy System Initiative: Air-Cooled Option RCCS Studies and NSTF Preparation", ANL-GenIV-179, Argonne National Laboratory Report.

[2] D. Lisowski, C. Gerardi, D. Kilsdonk, et al., 2016, "Progress Report on Water Conversion of the (NSTF) during FY2016," ANL-ART-69, Argonne National Laboratory Report.

[3] R. Hu, A. Kraus, M. Bucknor, Q. Lv, D. Lisowski, 2016, "Final Project Report on Computational Modeling and Analysis of Air-Based NSTF," ANL-ART-46, Argonne National Laboratory Report.

[4] R. Hu and W.D. Pointer, 2013, "CFD Analyses of Natural Circulation in the Air-Cooled Reactor Cavity Cooling System," Proc. International Conference on Mathematics and Computational Methods Applied to Nuclear Science & Engineering (M&C 2013).

[5] The RELAP5-3D Code Development Team, 2012, "RELAP5-3D Code Manual," INEEL-EXT-98-00834, Rev. 4, Idaho National Laboratory Report.

[6] CD-Adapco, 2015, "STAR-CCM+ 10.06 Manual."

[7] D. Lisowski, A. Kraus, M. Bucknor, R. Hu, and M. Farmer, 2016, "Experimental observations of natural circulation flow in the NSTF," *Nuclear Engineering and Design*, Vol. 306, 124-132.

[8] I.S. Walker and D.J. Wilson, "Evaluating Models for Superposition of Wind and Stack Effect in Air Infiltration," *Building and Environment*, Vol. 28, No. 2, pp. 201-210, 1993.

[9] F. P. Incropera and D. P. DeWitt., *Fundamentals of Heat and Mass Transfer*. New York: J. Wiley, 2002.

[10] The MathWorks, Inc., 2013, MATLAB and Statistics Toolbox Release 2013b, Natick, Massachusetts, United States.
[11] P. T. Tsilingiris, "Thermophysical and transport properties of humid air at temperature range between 0 and 100 °C," *Energy Conversion and Management,* Vol. 49, pp. 1098–1110, 2008.
[12] M. Bucknor, R. Hu, D. Lisowski, A. Kraus, 2016, "Comparisons of RELAP5-3D Analyses to Experimental Data from the Natural Convention Shutdown Heat Removal Test Facility", Proceedings of 2016 International Congress on Advances in Nuclear Power Plants (ICAPP'16).
[13] A. Kraus, R. Hu, D.D. Lisowski, M.D. Bucknor, 2016, "Turbulence Modeling Studies for Application to Buoyancy-Driven Air Flow Simulations of the NSTF," Proceedings of 11th Nuclear Reactor Thermal Hydraulics, Operation and Safety (NUTHOS-11).
[14] A. Kraus, R. Hu, D.D. Lisowski, M.D. Bucknor, 2016, "Simulation of Buoyancy-Driven Flow for Various Power Levels at the NSTF," Proceedings of 24th International Conference on Nuclear Engineering (ICONE-24).